Hemoglobin Kinetics and the Effect of Organic Phosphates

Abstract. *A kinetic model based on allosteric mechanisms of cooperativity fits the experimentally observed phosphate dependence of hemoglobin reactions. Subunit inequivalence is found to be important in analyzing hemoglobin kinetics. The observed increase in the rate of deoxygenation in the presence of organic phosphates is primarily related to the increased rate of dissociation of the second oxygen molecule.*

The kinetics of the reactions of hemoglobin (Hb) with ligands are generally interpreted by using an Adair scheme, with eight rate constants (1); this scheme applies to situations with rapid conformational equilibria and identical subunits. The Adair scheme, when extended to allow for inequivalent subunits (2), has 32 rate constants. Other kinetic models (3, 4) which are based on allosteric mechanisms for cooperativity do not allow for inequivalent subunits. All previous work has required a different set of rate constants for each set of experimental conditions (such as pH or phosphate concentrations).

The model we have developed (5) [based on a recently proposed equilibrium model (6)] allows for inequivalent subunits and combines different allosteric mechanisms for homotropic and heterotropic cooperativity. It is applied here to study the effect of 2,3-diphosphoglycerate (DPG), inositol hexaphosphate (IHP), and 8-hydroxy-1,3,6-pyrenetrisulfonate (HPT) on the kinetics of Hb deoxygenation and oxygenation. For a given phosphate a single set of parameters is sufficient to describe kinetic data over a wide range of phosphate concentrations.

The mechanism for homotropic cooperativity being considered corresponds to that of Perutz (7) (induced-fit binding of O_2 and conformational constraints), although we need not assume a fixed sequence of oxygenation, or a fixed point at which the quaternary conformation switches from the deoxy to the oxy form. The binding of organic phosphates is considered to shift the quaternary equilibrium and to alter the strength of the conformational (quaternary) constraints (6).

We assume that (i) the quaternary equilibrium and (ii) the equilibria of DPG, IHP, and HPT binding to Hb are rapid compared to the O_2 binding process. Evidence in support of (i) comes from flash photolysis experiments (8), while (ii) is consistent with the fact that preincubation of Hb with DPG (9) [or IHP (10) or HPT (11)] leads to the

same kinetics as observed when the two are mixed in a stopped-flow apparatus.

Figure 1A shows the equilibrium between the deoxy and oxy quaternary conformations of unliganded Hb, with equilibrium constant K_Q. Equilibria similar to that shown in Fig. 1A exist at every stage of ligand binding. The conformational equilibrium constant in the general case becomes

$$\frac{f_{ij}^{\text{deoxy},N}}{f_{ij}^{\text{oxy},N}} = K_Q \left(\frac{K_{\alpha,\text{deoxy},N}}{K_{\alpha,\text{oxy},N}}\right)^i \times \left(\frac{K_{\beta,\text{deoxy},N}}{K_{\beta,\text{oxy},N}}\right)^j \left(\frac{\tilde{K}_{\text{deoxy}}}{\tilde{K}_{\text{oxy}}}\right)^N \quad (1A)$$

Here f_{ij}^{QN} denotes the fraction of molecules that are in the Q quaternary conformation (Q = deoxy or oxy) and have N phosphate molecules bound ($N = 0$ or 1), i liganded α subunits, and j liganded β subunits ($i, j = 0, 1, 2$ for Hb); and $K_{\alpha,QN}$ denotes the equilibrium constant for ligand binding to an α subunit of a molecule in the Q quaternary con-

formation with N bound phosphate molecules. As shown in Fig. 1B, $\tilde{K}_{\text{deoxy}}$ and $\tilde{K}_{\text{oxy}}$ are the equilibrium constants for binding of organic phosphate, P, to unliganded Hb in the deoxy and oxy quaternary conformations, respectively. Equilibria similar to those shown in Fig. 1B exist at every stage of ligand binding, and the equilibria are described by equations analogous to Eq. 1A

$$\frac{f_{ij}^{Q1}}{f_{ij}^{Q0}} = [\text{P}]_{\text{free}}\tilde{K}_Q \left(\frac{K_{\alpha,Q1}}{K_{\alpha,Q0}}\right)^i \left(\frac{K_{\beta,Q1}}{K_{\beta,Q0}}\right)^j$$

(1B)

where the square brackets indicate concentration.

Figure 1C defines the off and on rate constants, $k_{\alpha,QN}$ and $k'_{\alpha,QN}$, for ligand binding to an α subunit of the Hb tetramer in the Q quaternary conformation with N phosphate molecules bound. The kinetics are obtained by using the "master equation" approach (4, 12), which allows us to decompose the off and on rates into equilibrium and kinetic factors

$$k'_{\alpha,QN} = [1 - \phi(Q)\theta_\alpha(N)]\omega_\alpha$$
$$k'_{\alpha,QN} = [1 + \phi(Q)\theta_\alpha(N)]\omega_\alpha K_\alpha \quad (1C)$$

(The rate constants for the β subunits can be similarly decomposed.) Here $\phi(Q) = \pm 1$ for the oxy and deoxy quaternary conformations, respectively;
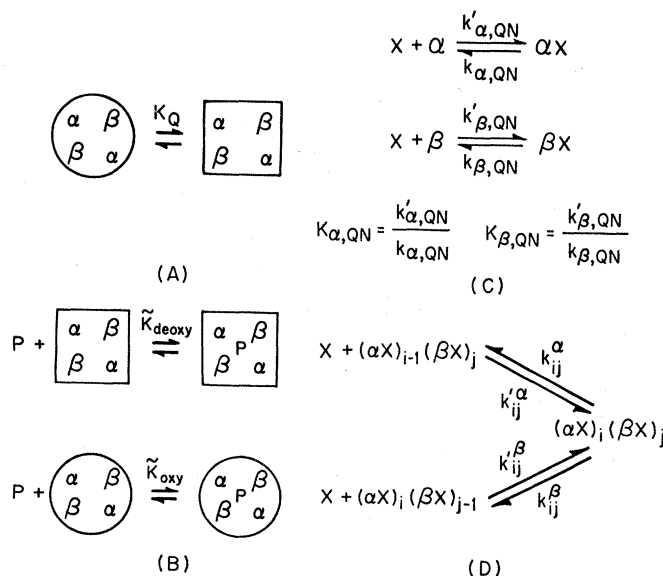

Fig. 1. The special case of the model which we apply here to Hb includes rapid quaternary conformation changes (A, short arrows), rapid phosphate binding (B, short arrows), and slow oxygen binding (C, long arrows). (A) Equilibrium between deoxy and oxy quaternary conformations of unliganded Hb, with equilibrium constant K_Q. (B) Equilibria for phosphate (P) binding to unliganded Hb in the deoxy and oxy quaternary conformation, with equilibrium constants $\tilde{K}_{\text{deoxy}}$ and $\tilde{K}_{\text{oxy}}$, respectively. (C) Reactions for ligand (X) binding to individual α and β subunits in a molecule which is in the Q (deoxy or oxy) quaternary conformation and has N (0 or 1) phosphate molecules bound. For the α subunits, the on and off rate constants are denoted by $k'_{\alpha,QN}$ and $k_{\alpha,QN}$, respectively, and the equilibrium constant by $K_{\alpha,QN}$. Similar notation is used for the β subunit. For a fixed phosphate concentration this model is equivalent to the extended Adair model (2) shown in (D). The overall rates k_{ij}^α, k'_{ij}^α, k_{ij}^β, and k'_{ij}^β are functions of the rate constants and equilibrium constants defined above.

$\theta_\alpha(N)$ is related to the strength of the quaternary constraints through $\theta_\alpha(N) \equiv \tanh[U_{QT}^\alpha(N)/k_BT]$, where k_BT is the product of the Boltzmann constant and the temperature, and $U_{QT}^\alpha(N)$ is the energy of the conformational constraints on an α subunit in the deoxy tertiary conformation when the molecule is in the oxy quaternary conformation (6). Therefore, $K_{\alpha,QN} \equiv k'_{\alpha,QN}/k_{\alpha,QN} = K_\alpha \exp[2\phi(Q)U_{QT}^\alpha(N)/k_BT]$, consistent with equations 34 and 37 of (6). Note that in the absence of quaternary constraints, $\theta_\alpha(N) = 0$ and K_α is the equi-

librium constant for induced-fit binding of the ligand to a single α subunit. If $\theta_\alpha(1) = \theta_\alpha(0)$, then the organic phosphate does not alter the strength of the quaternary constraints and its inhibitory effect is solely due to its preferential binding to the two quaternary conformations. The parameter ω_α has no equilibrium analog; it represents the off rate from an α subunit in the absence of quaternary constraints. In principle, ω_α could be dependent on the quaternary state and the presence of effectors. These possibilities have been systematically

explored in fitting the theory to experimental data.

If the α and β subunits are considered kinetically equivalent, then $k'_{oxy,N=0}$ and $k_{oxy,N=0}$ can be estimated by measuring the rate constants for the binding of the fourth ligand molecule in the absence of phosphates. Similarly, $k'_{deoxy,N=0}$ and $k_{deoxy,N=0}$ can be obtained from the rate constants for the binding of the first ligand molecule (3). Estimates of $k'_{Q,N=1}$ can be similarly obtained from analyzing the reactions at very high organic
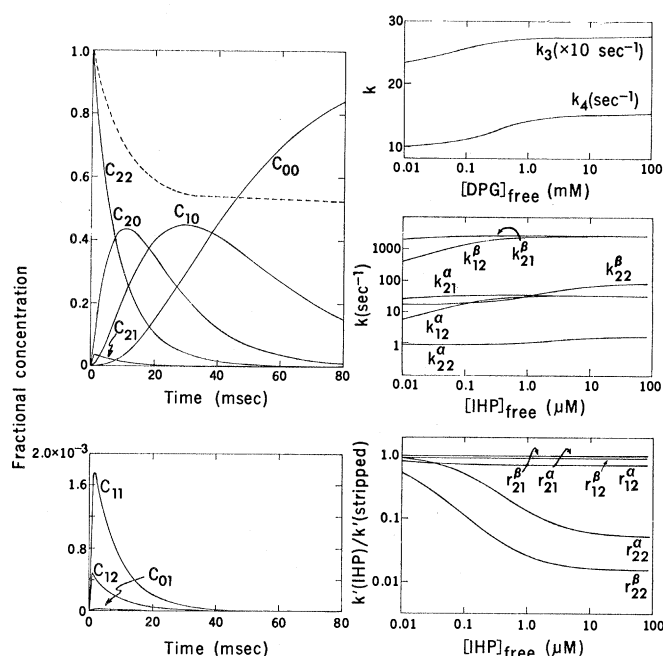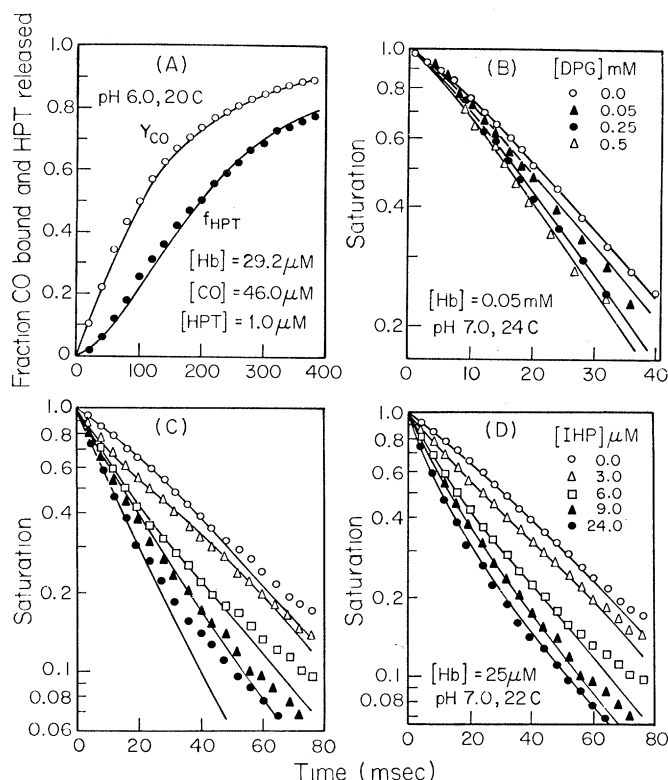

Fig. 2 (left). Experimental data points compared with theoretical kinetic curves. (A) Data of MacQuarrie and Gibson (11) for CO binding and HPT release; $Y_{CO} \equiv$ fractional saturation with CO, and $f_{HPT} \equiv$ fraction of HPT released. Solid curves were calculated assuming identical subunits ($\alpha = \beta$), with $\omega_\alpha K_\alpha = 9.8$ liter μmole^{-1} sec^{-1}, $\theta_\alpha = 0.9848$, $K_Q = 2.71 \times 10^{12}$, $\tilde{K}_{oxy} = 5.26 \times 10^4$ liter/mole, and $\tilde{K}_{deoxy} = 9.1 \times 10^4$ liter/mole. (B) Data of Salhany et al. (13) for deoxygenation of oxy-Hb by dithionite in the presence of DPG. Curves were calculated assuming identical subunits, with $\omega_\alpha = 147.5$ sec^{-1}, $\theta_\alpha = 0.9403$, $K_Q = 4.468 \times 10^9$, $\tilde{K}_{oxy} = 3.2 \times 10^3$ liter/mole, and $\tilde{K}_{deoxy} = 2.13 \times 10^4$ liter/mole. (C) Data of Gray and Gibson (10) for deoxygenation of oxy-Hb by dithionite (Na$_2$S$_2$O$_4$) in the presence of IHP. Theoretical curves were calculated with $\omega_\alpha = 556$ sec^{-1}, $\theta_\alpha = 0.9866$, $K_Q = 3.08 \times 10^{11}$, $\tilde{K}_{oxy} = 0.94 \times 10^5$ liter/mole, and $\tilde{K}_{deoxy} = 7.26 \times 10^5$ liter/mole. (D) Reaction of Fig. 2C calculated by assuming inequivalent subunits ($\alpha \neq \beta$). The theoretical parameters are $\omega_\alpha = 18$ sec^{-1}, $\omega_\beta = 1384$ sec^{-1}, $\theta_\alpha(0) = \theta_\alpha(1) = 0.9496$, $\theta_\beta(0) = \theta_\beta(1) = 0.9873$, $K_Q = 5.327 \times 10^{10}$, $\tilde{K}_{oxy} = 2.69 \times 10^5$ liter/mole, and $\tilde{K}_{deoxy} = 1.83 \times 10^8$ liter/mole. In the data shown in (C) and (D) some of the Hb may be present as dimers (< 10 percent, using [Hb] $= 50 \mu M$ before mixing). With increasing IHP, the fraction of dimers will decrease. The disagreement between calculation and experiment near the end of the reaction could be partly due to slow absorbance changes involving dimers. Fig. 3 (right). Time dependence of the concentrations of the various species produced in the reaction of Fig. 2, C and D, and the effect of organic phosphates on the rate constants. (A) Fractional concentrations of various liganded species, $C_{ij} = [(\alpha x)_i(\beta x)_j]/[Hb_i]_{total}$ and [IHP]$_{free}$/[IHP]$_{free\ at\ t=0}$ (dashed line) as a function of time, calculated by using the parameter values of Fig. 2D. Total IHP $= 9.0 \mu M$ and total Hb$_4 = 6.25 \mu M$ (by tetramer). The value of C_{02} is less than 10^{-5} and cannot be displayed on either scale. (B, top) Dependence of k_4 and k_3 on [DPG]$_{free}$, calculated by using the parameters of Fig. 2B. The rates $k_1 = k_2 = 286$ sec^{-1} were not significantly increased (see text). (B, middle) Effect of [IHP]$_{free}$ on the off rates k_{22}, k_{21}, and k_{12} for the α and β subunits, calculated from the parameters of Fig. 2D. The subunit with the greater value of k_{22} is identified as the β subunit, in accordance with previous findings (18). Here again, the off rates from species with at most two hemes liganded are not significantly altered by IHP; $k_{10}^\alpha = k_{20}^\alpha = k_{11}^\alpha = 35.6$ sec^{-1}; $k_{01}^\beta = k_{02}^\beta = k_{11}^\beta = 2750$ sec^{-1}. (B, bottom) Calculated variation in the ratio $r_{ij}^\alpha \equiv k'^\alpha_{ij}$ (IHP)$/k'^\alpha_{ij}$ (IHP $= 0$), and $r_{ij}^\beta \equiv k'^\beta_{ij}$ (IHP)$/k'^\beta_{ij}$ (IHP $= 0$) with [IHP]$_{free}$, for $i + j \geq 3$. This prediction should be amenable to experimental verification. The concentration of DPG is in millimoles per liter and that of IHP in micromoles per liter. All rate constants are expressed on a per heme basis. We have calculated the relative probabilities of the deoxy and oxy quaternary conformations in the Hb molecule with n hemes deoxygenated. Using the theoretical parameters given in Fig. 2B for DPG and in Fig. 2D for IHP, we find that the switch from the oxy to the deoxy quaternary conformation occurs just after or just before the deoxygenation of the second heme, depending on the phosphate concentration. Thus the change in k_{21}, k_{12}, and k'_{22} (for both α and β subunits) with increasing phosphate concentration is related to the fact that the presence of phosphates has its strongest effect on the quaternary conformation of Hb with three hemes liganded.

phosphate concentrations. These estimates of $k'_{Q,N}$ and $k_{Q,N}$ can, in principle, be used to determine the parameters ω, K, and $\theta(N)$. For the case of inequivalent subunits, estimates of $k'_{\alpha,QN}$ and $k_{\alpha,QN}$ would be required to determine ω_α, K_α, and $\theta_\alpha(N)$. The organic phosphate binding constants $\tilde{K}_{\text{oxy}}$ and $\tilde{K}_{\text{deoxy}}$ can be obtained by direct measurement (10, 11). The remaining parameter, K_Q, can be obtained from fitting equilibrium oxygenation data (3). For the kinetic data analyzed here, we have determined all the parameters by a least squares fitting procedure.

Figure 2A shows data (11) for the binding of CO and consequent release of HPT, a fluorescent analog of DPG. By treating the subunits as equivalent and neglecting the CO off rates, we can fit both sets of data to better than 1 percent per point by using a single set of five parameters ($\omega_\alpha K_\alpha$ θ_α, K_Q, $\tilde{K}_{\text{ovr}}$, and $\tilde{K}_{\text{deoxy}}$); here $\theta_\alpha \equiv \theta_\alpha(1) = \theta_\alpha(0)$. MacQuarrie and Gibson (11) require nine parameters to explain these data—four CO rate constants and five HPT equilibrium constants.

Figure 2B shows data (13) for the release of O_2 from oxy-Hb in the presence of varying DPG concentrations. The $[O_2]_{\text{free}}$ at $t = 0$ and $[\text{Na}_2\text{S}_2\text{O}_4]$ were such that $[O_2]_{\text{free}}$ becomes negligible in < 5 msec (14). Thus, only the off rates contribute to the reaction. The five parameters (ω_α, θ_α, K_Q, $\tilde{K}_{\text{oxy}}$, and $\tilde{K}_{\text{deoxy}}$) were found from the fit to the data for 0 and 0.5 mM DPG, and these same parameters were then used to calculate the curves for 0.05 and 0.25 mM DPG. The agreement of these calculated curves with the data gives us confidence in the predictive ability of our approach. No further improvements in fit were obtained by considering the possibilities of (i) inequivalent subunits ($\alpha \neq \beta$), (ii) DPG having an effect on the quaternary constraints, and (iii) the time scaling parameter, ω, being dependent on the quaternary conformation or DPG binding. Note that the Adair scheme (1) requires four off rate constants for *each* DPG concentration, making a total of 16 parameters for the data of Fig. 2B. If the equilibrium scheme of Tyuma *et al.* (15) is extended to kinetics, a total of 13 parameters is required for the deoxygenation data, and a total of 21 parameters for oxygenation data.

Figure 2, C and D, show deoxygenation data (10) in the presence of IHP.

A slight improvement over the five-parameter fit (Fig. 2C) was obtained by considering IHP to alter the quaternary constraints, whereas the effects of considering ω_α and ω_β to depend on quaternary conformation and IHP binding were insignificant. A somewhat improved fit (Fig. 2D) was obtained by allowing for $\alpha \neq \beta$ (seven parameters). These results suggest that the α and β subunits may be kinetically inequivalent in the presence of IHP. That this inequivalence does not appear with DPG may be due to the fact that DPG does not affect the limiting rate constant $k_4 = (k_{22}^\alpha + k_{22}^\beta)/2$, whereas IHP does.

Figure 3A shows the time dependence of $[\text{IHP}]_{\text{free}}$ and the concentrations of the variously liganded species produced in the course of the reaction. Note that the concentrations of the intermediate species are very small when compared with the fully liganded and fully unliganded species. A comparison of the fraction of O_2 released with the fraction of IHP bound, at every instant of time, shows that the release of O_2 lags behind the binding of IHP. This lag is related to the switchover to the deoxy conformation when only three hemes are liganded. (The same effect is less pronounced for DPG.) This result agrees with the similar prediction for DPG based on ^{31}P nuclear magnetic resonance spectra (16), as well as with the results shown in Fig. 2A (11).

The kinetic equations for the model shown in Fig. 1 reduce to the Adair form (1, 2) when the conformational equilibria and the organic phosphate binding equilibria are rapid. If $\alpha \neq \beta$, the 32 rate constants of the Olson-Gibson reaction scheme (2) are given by

$$k_{ij}^\alpha = \sum_Q \sum_{N=0}^{1} f_{ij}^{QN} \, k_{\alpha,QN}$$

$$k'^{\alpha}_{ij} = \sum_Q \sum_{N=0}^{1} f_{i-1,j}^{QN} \, k'_{\alpha,QN} \qquad (2)$$

where $i = 1, 2$ and $j = 0, 1, 2$. The rates k_{ij}^β and k'^{β}_{ij} can be expressed similarly. The f_{ij}^{QN} can be obtained from Eqs. 1A and 1B by applying the constraint $\Sigma_Q\Sigma_N f_{ij}^{QN} = 1$. [All rate constants are expressed on a per heme rather than a per tetramer basis (2).] If $\alpha = \beta$, the eight off and on rates, k_n and k'_n ($n = 1$, . . . , 4), for the $\alpha = \beta$ Adair scheme (1) are obtained from Eq. 2 by setting $k_{n=i+j} = k_{ij}^\alpha$, $k'_{n=i+j} = k'^{\alpha}_{ij}$, and $f_n^{QN} = \Sigma_{i,j}^{i+j=n} f_{ij}^{QN}$. Thus at a fixed phosphate concentration these eight rate constants can be expressed as functions

of the four parameters ω, $\theta(0)$, K, and K_Q. If $\alpha \neq \beta$, the 32 rate constants can be expressed as functions of the seven parameters ω_α, ω_β, $\theta_\alpha(0)$, $\theta_\beta(0)$, K_α, K_β, and K_Q. In addition, for a rapidly equilibrating phosphate, the parameters $\tilde{K}_{\text{oxy}}$, $\tilde{K}_{\text{deoxy}}$, $\theta_\alpha(1)$, and $\theta_\beta(1)$ are sufficient to describe the phosphate dependence of the rate constants.

Experiments show that the overall dissociation velocity increases in the presence of organic phosphates. Since the reaction consists of many steps it is not possible to tell experimentally which step is most affected by phosphates. However, a theoretical analysis of the data can be used to predict which step is affected most. For this purpose the phosphate dependence of the Adair rate constants is calculated and the results are shown in Fig. 3B. Whereas DPG causes only a small increase in k_4, IHP has a significant effect on k_{22}^β. The largest effect of phosphates is on the off rate for the release of the second O_2 molecule from fully liganded Hb (that is, k_3 or k_{21} and k_{12}). In the case of IHP, with inequivalent subunits ($\alpha \neq \beta$), the increase is greatest for dissociation from the species with one α and two β subunits liganded. It is the dependence of k_{22}, k_{21}, and k_{12} on $[\text{IHP}]_{\text{free}}$ which causes biphasic deoxygenation when $[\text{IHP}]_{\text{free}}$ decreases significantly during the reaction.

If the phosphates do not alter the quaternary constraints and the kinetic parameter ω, then k_{10}^α and k_{01}^β would not be significantly altered by these effectors. Hence dependence of these rate constants (and the equilibrium constants K_{10}^α and K_{01}^β) on phosphate concentration would indicate an effect of phosphates on the strength of the quaternary constraints and the parameter ω. The calculations show that the k_{ij} with $i + j \leq 2$ are at least an order of magnitude larger than k_{22}^α and k_{22}^β. Since in the experiments analyzed here only very small quantities of partially liganded species are produced, k_{ij} ($i + j \leq 2$) cannot be determined very accurately.

The ratio of the on rates k'_{ij} (phosphates)$/k'_{ij}$ (stripped) can be calculated by using the parameters determined here. This ratio decreases as phosphate concentration increases, in agreement with the results of Gibson (17). As can be seen from Fig. 3B, k'^{β}_{22} decreases most, and k'^{α}_{22} and k'^{α}_{12} decrease somewhat less. The decrease of k'^{α}_{22} and k'^{β}_{22} in the presence of IHP agrees with the measured decrease in

k'_4 (10). In contrast to the result of Gibson (17), we find that k'_4 decreases with increasing DPG.

The results of our calculation show that (i) the major kinetic effects of different quaternary conformations and of phosphate binding are reproduced sufficiently well by considering simply quaternary constraints and preferential binding; (ii) the inequivalence of subunits ($\alpha \neq \beta$) is important in analyzing deoxygenation data in the presence of IHP; (iii) the observed increase in the "overall" deoxygenation rate in the presence of IHP largely results from the increase in the rate of dissociation of the second molecule, and this is related to the switchover to the deoxy quaternary conformation at this stage of the reaction; (iv) the calculated values of $\tilde{k}_4$, $\tilde{k}_{22}^\beta$, and the binding constants K_{oxy} and K_{deoxy} for HPT, DPG, and IHP are in agreement with previously determined values (10, 11, 17, 18); and (v) our value of k_{22}^α is somewhat lower than that determined by Olson et al. (18). While we believe that k_3 is well determined in this analysis, the values of k_1 and k_2 can only be considered to be estimates. Our results point to the need for an accurate set of data at various DPG (or IHP) levels from O_2 binding experiments and from experiments where significant quantities of intermediates are produced (19). The successful use of the master equation formulation to predict the kinetics of hemoglobin reactions suggests the possible use of this approach to the kinetics of other cooperative proteins.

RAMA BANSIL*, JUDITH HERZFELD†
H. EUGENE STANLEY

Harvard–MIT Program in
Health Sciences and Technology and
Department of Physics,
Massachusetts Institute of
Technology, Cambridge 02139

References and Notes

1. Q. H. Gibson and F. J. W. Roughton, Proc. R. Soc. Lond. Ser. B Biol. Sci. 146, 206 (1957).
2. J. S. Olson and Q. H. Gibson, J. Biol. Chem. 247, 1713 (1972).
3. J. J. Hopfield, R. G. Shulman, S. Ogawa, J. Mol. Biol. 61, 425 (1971).
4. R. T. Bush and C. J. Thompson, Biopolymers 10, 961 and 1331 (1971).
5. R. Bansil, thesis, University of Rochester (1974).
6. J. Herzfeld and H. E. Stanley, J. Mol. Biol. 82, 231 (1974); Biochem. Biophys. Res. Commun. 48, 307 (1972).
7. M. F. Perutz, Nature (Lond.) 228, 726 (1970).
8. B. Alpert, R. Banerjee, L. Lindqvist, Proc. Natl. Acad. Sci. U.S.A. 71, 558 (1974); J. A. McCray, Biochem. Biophys. Res. Commun. 47, 187 (1972).
9. Q. H. Gibson, Biochem. Biophys. Res. Commun. 40, 1319 (1970).
10. R. D. Gray and Q. H. Gibson, J. Biol. Chem. 246, 7168 (1971).
11. R. MacQuarrie and Q. H. Gibson, ibid. 247, 5686 (1972).
12. R. J. Glauber, J. Math. Phys. 4, 294 (1963). For applications of this approach to cooperative phenomena in other systems, see, for example, H. E. Stanley, Introduction to Phase Transitions and Critical Phenomena (Oxford Univ. Press, London, 1971).
13. J. M. Salhany, R. S. Eliot, H. Mizukami, Biochem. Biophys. Res. Commun. 39, 1052 (1970).
14. The upper limit of 5 msec is arrived at by assuming that the reaction of O_2 with $Na_2S_2O_4$ is zero order in O_2 and first order in $Na_2S_2O_4$ [J. A. Morello, M. R. Craw, H. P. Constantine, R. E. Forster, J. Appl. Physiol. 19, 522 (1964)] with rate constant $k = 1.7$ sec^{-1} at pH 8.0 [D. O. Lambeth and G. Palmer, J. Biol. Chem. 248, 6095 (1973)] and higher at pH 7.0 [H. Hartridge and F. J. W. Roughton, Proc. R. Soc. Lond. Ser. A Math. Phys. Sci. 104, 395 (1923)].
15. I. Tyuma, K. Imai, K. Shimizu, Biochemistry 12, 1491 (1973).
16. W. H. Heustis and M. A. Raftery, Biochem. Biophys. Res. Commun. 49, 428 (1972).
17. Q. H. Gibson, J. Biol. Chem. 245, 3285 (1970).
18. J. S. Olson, M. E. Anderson, Q. H. Gibson, ibid. 246, 5919 (1971).
19. Q. H. Gibson, Proc. Natl. Acad. Sci. U.S.A. 70, 1 (1973); Y. Henry and R. Cassoly, Biochem. Biophys. Res. Commun. 51, 659 (1973); R. Cassoly, ibid. 55, 1208 (1973).
20. We thank J. M. Salhany, R. D. Gray, and Q. H. Gibson for providing their raw data and for helpful discussions. Supported by the Research Corporation and by NIH grant HL 14322-02 (R. W. Mann, principal investigator).
* Present address: Gordon McKay Laboratories, Harvard University, Cambridge, Mass. 02138.
† Present address: Biophysical Laboratory, Harvard Medical School, Boston, Mass. 01451.

8 July 1974; revised 10 September 1974 ∎

Negative Resistance Characteristic Essential for the Maintenance of Slow Oscillations in Bursting Neurons

Abstract. Voltage clamping giving step commands reveals a steady-state negative resistance characteristic in the current-voltage curves of Aplysia bursting neurons. This is observed below spike threshold in the unstable range through which the membrane potential slowly oscillates. The negative resistance characteristic underlies this instability and shapes the rapid depolarization-hyperpolarization phase of the cycle. When bursting cells are converted to silent cells (by cooling) the negative resistance is abolished; conversely, when normally silent cells are made to burst (by warming) a negative resistance develops. The presence of negative resistance thus enables the bursting cell to oscillate, whereas its absence precludes such oscillations.

Bursting neurons of the marine mollusk Aplysia californica show a remarkable voltage instability within their range of oscillation. It is impossible, by injecting steady currents, to stabilize the membrane potential of a bursting cell between the extremes of its cycle. The membrane potential will come to a steady value only at the top of the range (with the cell firing steadily), or near the most hyperpolarized point. Studies by Carnevale and Wachtel (1) demonstrated the presence of a steady inward current which depolarizes a bursting cell, and a transient outward current which, triggered by the depolarization, temporarily hyperpolarizes the neuron. However, the simple combination of these reciprocating membrane currents does not explain the voltage instability of these cells. Such a model would be expected to stabilize at any potential within the oscillating range if one injected sufficient hyperpolarizing current to counter the depolarizing influence.

In order to elucidate the mechanisms specifically underlying the oscillations, we took advantage of the fact that the cycle can be reversibly blocked by cooling (2). When the temperature of the ganglion is reduced from 22° to 10°C, the intrinsic region of voltage instability is often eliminated, and a stable resting potential is established near the top of the oscillation range. To explore fully the essential features distinguishing warm bursting cells from cells silenced by cooling, we used the voltage clamp technique to examine the current-voltage (I-V) relation of the same cell under both temperature conditions. Intracellular recordings were made from abdominal ganglion bursting cells (L_2 to L_6) by using two KCl-filled microelectrodes and standard techniques (3). Our voltage clamp was designed to study small currents (0.1 na) below spike threshold. Axonal charging currents prohibited the study of events shorter than 100 msec (4), but this response time was sufficient to register the slow currents underlying the oscillation.

We adjusted the voltage clamp to hold the cell at the least negative point in the cycle of oscillation (usually between −25 and −30 mv). When the clamp was activated, the holding current achieved a steady inward value